Original Article

Continuous heating transformation diagram and austenitic grain refinement in a commercial brazilian boron steel

Alice Silva Gonçalves [1]
Paulo Sérgio Moreira [1]
Geraldo Lúcio de Faria [1*]

Abstract

Although conventional heat treatment methods have been widely employed for decades, their limitations have become increasingly evident, particularly regarding energy inefficiency, high operational costs, and emissions associated with long heating and cooling cycles. In this context, fast-heating techniques such as Ultra-Fast Heating (UFH) have emerged as promising alternatives by combining sustainability, high productivity, and the potential for microstructural refinement, which can lead to superior mechanical properties in steels. This study aimed to determine the Continuous Heating Transformation (CHT) diagram and to evaluate the effect of heating rate on the austenitic grain size (AGS) of a commercial Brazilian boron steel. Dilatometric tests were performed under different heating rates to determine the critical austenitizing temperatures (Ac_1 and Ac_3) and to construct the corresponding CHT diagram. Additionally, microstructural analyses were carried out to reveal and quantify the AGS for each condition. The results showed that increasing the heating rate shifts the critical transformation temperatures to higher values, highlighting the kinetic effects on phase transformations. Moreover, higher heating rates promoted significant grain refinement, reducing the average grain size from approximately 60 μm to about 10 μm solely through thermal control. These findings demonstrate the potential of UFH as an effective tool for microstructural engineering, enabling the optimization of mechanical properties while improving the energy efficiency of industrial heat treatment processes.

Keywords: CHT diagram; Heating rate; Grain refinement; Boron steel.

1 Introduction

Despite the consolidated use of conventional heat treatment methodologies in sectors such as automotive, naval, oil & gas, and civil construction, some of their limitations have become increasingly evident. Although these methods are effective in achieving the desired results, they present significant challenges, including energy inefficiency, high operational costs, and carbon emissions associated with relatively long heating and cooling cycles [1]. In addition, the thermal gradients often generated during processing may lead to distortions and non-uniform properties in large components, which require additional machining and processing steps. Longer processing time intervals also increase material waste, thereby compromising resource efficiency as well as economic and environmental sustainability [2,3].

In this context, the search for more efficient and sustainable alternatives has driven the development of techniques based on induction or electrical resistance heating, such as Ultra-Fast Heating (UFH). This UFH methodology is distinguished by the possibility to provide fast and homogeneous heating of thin components, significantly reducing thermal cycle duration, energy consumption, and thermal gradients. In addition to improving productivity, UFH minimizes distortions and enhances the final quality of materials [1]. Thus, it represents an approach that is aligned with the growing demand for industrial sustainability, contributing to the decrease in carbon emissions.

UFH has gained prominence not only for its operational and energy-related benefits but also for enabling significant advances in microstructural refinement. The high heating rate, which is a key feature of this technique, increases the density of sites available for austenite nucleation while simultaneously limiting the time available for austenitic grain growth. As a result, more refined microstructures can be obtained, enhancing mechanical properties such as tensile strength and ductility. The literature highlights that UFH can be effective in refining the microstructure of Dual-Phase (DP) steels, widely used as thin sheets, and can also be applied to develop ultrafine-grained products, reducing processing time without compromising the balance between mechanical strength and ductility [4,5].

Historically, the development of Advanced High-Strength Steels (AHSS) has been primarily based on controlling the cooling rate and on the addition of alloying elements. However, techniques such as UFH have been investigated to enhance the mechanical properties of these materials through the manipulation of parameters such as heating rate and microstructural control, even enabling the reduction of certain alloying additions depending on the targeted product class [6]. In addition to its energy efficiency, UFH has shown a positive impact on the mechanical performance of medium-carbon steels, DP steels, Q&P (Quenching and Partitioning) steels, among others. Recent studies indicate that heating rates above 100 °C/s promote severe grain refinement, increase the critical transformation temperatures (Ac_1 and Ac_3), and raise the superheating degree of the austenitic transformation. These changes enhance the austenite nucleation rate, leading to improved mechanical strength and elongation of the processed materials [7,8]. Thus, ultra-fast heating emerges as a viable and sustainable alternative to conventional methods, combining energy efficiency, microstructural refinement, and superior mechanical performance. Its versatility across different alloys and geometries, together with the potential to reduce emissions and enhance productivity, highlights UFH as a methodology well-suited to address current industrial demands focused on sustainability and advanced material performance. Consequently, in recent years, UFH has increasingly attracted the attention of researchers worldwide [1,4-8].

There is consensus in the literature that the heating rate influences both the kinetics of austenite formation and microstructural refinement, since this parameter governs diffusional and/or massive mechanisms involved in the process [9-14].

At low heating rates, austenite formation is controlled by carbon diffusion, whereas at higher heating rates, it is governed by interface migration.

Recently, Oliveira et al. [9] reported that the use of UFH has the potential to refine the austenitic grain size in a TRIP780 steel, provided that soaking conditions are properly controlled. According to the literature, increasing the heating rate raises the superheating degree of the initial structure. In this case, the driving force for austenite formation increases significantly, while the critical embryo size and the energy required for its formation decrease, thereby promoting the generation of a greater number of austenite nuclei in the material's microstructure. Consequently, since each nucleus formed with a radius equal to or greater than the critical size evolves into a grain, the austenite produced upon reaching the Ac_3 temperature tends to exhibit microstructures with smaller grains [10,15,16]. However, when the heating rate is combined with a prolonged soaking time at the peak temperature, and if the material does not contain mechanisms capable of restricting grain growth, grain coarsening is expected to occur, thereby eliminating the refinement achieved at the Ac_3 temperature [4,9,17,18]. Accordingly, Oliveira et al. [9] justified the absence of a significant effect on the austenitic grain size of a TRIP780 steel when subjected to relatively long soaking times. This finding indicates that each steel may exhibit a particular behavior regarding the effects of these parameters.

Considering these aspects, a comprehensive understanding of the influence of heating rate on austenite formation is essential, since the resulting austenitic grain size directly governs the morphology of subsequent constituents such as ferrite, pearlite, bainite, and martensite. As finer austenitic grains generally promote simultaneous improvements in both strength and toughness, UFH appears particularly promising as a tool for microstructural refinement through controlled heating conditions. In this context, the present study focuses on a commercial Brazilian boron steel, aiming to construct its Continuous Heating Transformation (CHT) diagram and to evaluate the extent to which increasing heating rates affect the as-received structure superheating and the austenite grain size refinement. The evaluated steel is widely used in applications that combine the need for high mechanical strength with good toughness, such as agricultural disks subjected to severe impact loading. Therefore, this first investigation provides valuable insights into the potential of heating rate control as a strategy to optimize heat treatment parameters in order to refine the martensitic microstructure obtained after quenching and, ultimately, to enhance the mechanical performance of boron steels.

2 Materials and methods

In this study, a modified SAE 15B30 (higher Mn content) steel was used, and its chemical composition is presented in Table 1. The material was obtained from a hot-rolled strip with a thickness of approximately 6 mm, processed by thermomechanical rolling. Samples were extracted from this strip and machined into dilatometry specimens, which initially exhibited a microstructure composed of ferrite and pearlite. The specimens were machined into solid cylinders with dimensions of 10 mm in height and 3 mm in diameter. The machining was carried out in such a way that the height of all specimens was always aligned with the strip rolling direction.

The evaluation of the heating rate effect on this steel austenitizing kinetics was previously detailed by Gonçalves et al. [15].

In the present work, aiming to extend this analysis by determining the critical transformation temperatures (Ac_1 and Ac_3) and constructing the Continuous Heating Transformation

Table 1. Chemical composition (wt.%) of the commercial boron steel evaluated in this study

C	Mn	Si	P	S	Al	Nb	Ti	Cu	B	V	Ni	Cr	Mo	N
0.29	1.24	0.23	0.019	0.008	0.033	0.001	0.029	0.01	0.0032	0.005	0.01	0.23	0.002	0.0053

(CHT) diagram, nine dilatometry specimens were subjected to different heating rates up to 1150 °C, held for 1 second, and then cooled to room temperature at 200 °C/s under a controlled flow of analytical-grade helium gas (5.0). The heating rates investigated were: 0.10, 1, 3, 5, 15, 30, 50, and 100 °C/s. All experiments were performed using a LINSEIS R.I.T.A. L78 quenching dilatometer.

For the precise determination of the critical transformation temperatures Ac_1 and Ac_3, the minimum deviation method was applied, which required defining the linear regions preceding and following steel austenitizing. In this context, the nine initial dilatometry specimens were heated up to 1150 °C to ensure accurate identification of Ac_3. However, under such conditions, there was a possibility of austenitic grain growth, making it difficult to ascertain whether the effect of heating rate on grain refinement would be retained at the end of austenitization. To address this concern, three complementary experiments were carried out by heating specimens from room temperature to a lower austenitizing temperature, at heating rates of 3, 30, and 100 °C/s. After holding for 1 second, the samples were cooled to room temperature at 200 °C/s under a controlled flow of analytical-grade helium gas (5.0), in order to obtain predominantly martensitic microstructures. This microstructural condition was essential for the effectiveness of the oxidation-etching technique used to reveal prior austenite grain boundaries [19-21].

After completing the heat treatments, for each heating rate investigated, the dilatation data (ΔL) as a function of temperature (T), recorded by the dilatometer software during continuous heating, were collected and transferred to OriginPro 9.0. In this software, dilatometric curves of relative length ($\Delta L/L_0$) as a function of temperature (T) were plotted, where L_0 corresponds to the initial height of the specimen. The minimum deviation method was then applied to determine the critical transformation temperatures, namely the beginning (Ac_1) and the end (Ac_3) of steel austenitizing, for each heating rate. Subsequently, the Continuous Heating Transformation (CHT) diagram for the studied steel was constructed. To this end, the experimental data previously determined by Gonçalves et al. [15] were compiled, including the critical austenitic transformation temperatures (Ac_1 and Ac_3) and the corresponding times to reach these temperatures (tAc_1 and tAc_3), based on Equation 1. Where ΔT is the temperature variation, Δt is the time variation, T_f is the final temperature (Ac_1 or Ac_3), T_i is the initial temperature (standardized as 25 °C), t_f is the final time (required to reach Ac_1 or Ac_3), and t_i is the initial time (standardized as 0 seconds). By substituting the standardized variables (T_i and t_i) and isolating t_f, Equation 2 is obtained.

Thus, to calculate the time required to reach the critical temperature Ac_1, it is sufficient to replace t_f and T_f in Equation 2 with tAc_1 and Ac_1, respectively. This leads to Equation 3. Similarly, to calculate the time required to reach the critical temperature Ac_3, it is sufficient to replace t_f and T_f in Equation 2 with tAc_3 and Ac_3, respectively. Therefore, Equation 4 is obtained.

$$Rate = \frac{\Delta T}{\Delta T} = \frac{Tf - Ti}{Tf - ti} \tag{1}$$

$$tf = \frac{Tf - 25}{Taxa} \tag{2}$$

$$tAc1 = \frac{Ac1 - 25}{Taxa} \tag{3}$$

$$tAc3 = \frac{Ac3 - 25}{Taxa} \tag{4}$$

To reveal the prior austenite grains, the samples, after standard metallographic preparation, were subjected to an oxidation heat treatment in a tubular furnace with an inert atmosphere [14,18,20,21]. In this process, the specimens were heated to the selected oxidation temperature, ranging between 640 °C and 660 °C. It is noteworthy that in all tests the oxidation temperature was kept below the austenitizing start temperature (Ac_1) of the steel, thus characterizing a subcritical oxidation heat treatment. After reaching the oxidation temperature, the samples were held for 12 minutes and subsequently cooled to room temperature under a controlled argon flow. Subsequently, for each oxidized specimen, 10 optical micrographs were acquired at 200× magnification for the quantification of prior austenite grain size (PAGS).

The PAGS measurement was carried out using the linear intercept method, as described in ASTM E112-13 [22]. This technique consists of superimposing test lines on the micrographs obtained by optical microscopy, followed by measuring the total line length and counting the intercepts between the lines and the grain boundaries. Considering the predominantly equiaxed morphology of the observed austenite grains, only horizontal lines were used to ensure adequate statistical representativeness. For each evaluated condition, five micrographs acquired from different fields of the sample were analyzed to account for possible local microstructural variations. In each image, at least five test lines were applied, totaling a minimum of 25 lines analyzed per heating condition. All results obtained showed a relative precision better than 10%, meeting the reliability criteria established by ASTM E112-13 [22].

3 Results and discussion

3.1 Continuous Heating Transformation (CHT) diagram

Figure 1 shows the Continuous Heating Transformation (CHT) diagram for the evaluated steel, determined from the dilatometric data obtained under different heating rates. The analysis of this diagram is essential to understand the material austenitizing behavior under variable thermal conditions, particularly in industrial processes that involve continuous heating cycles. The CHT diagram illustrates the evolution of the critical transformation temperatures Ac_1 (onset of austenite formation) and Ac_3 (completion of
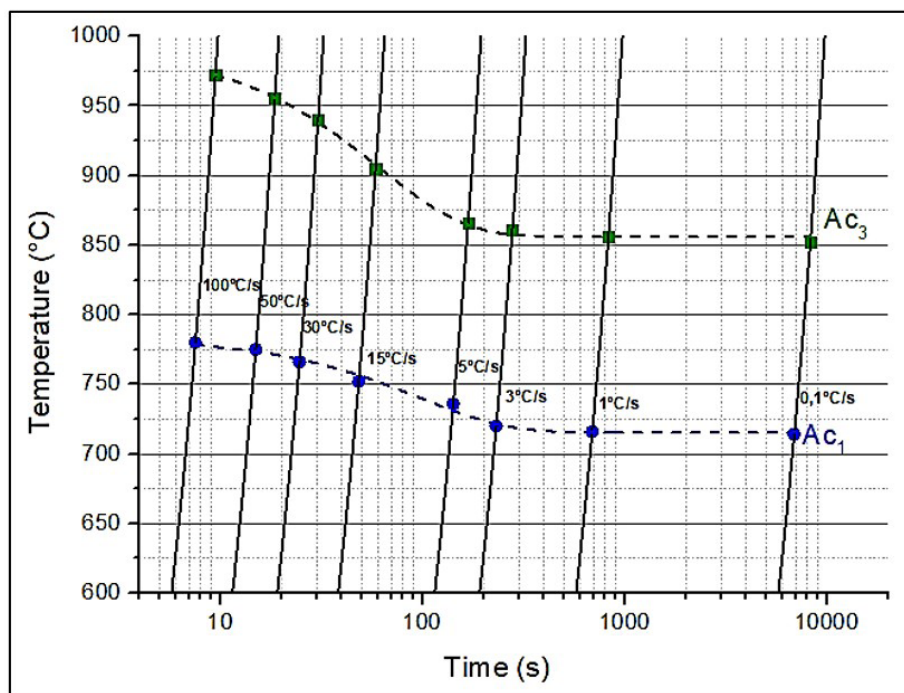
Figure 1. Continuous Heating Transformation (CHT) diagram of the studied SAE 15B30 steel, obtained from an initial microstructure composed of ferrite and pearlite.

steel austenitizing) as a function of the time required to reach them during continuous heating. The results show that, with increasing heating rate, both Ac_1 and Ac_3 temperatures shift to higher values, a trend already reported in the literature for different classes of steels [9,14,18].

For the investigated steel, this effect is particularly more pronounced for Ac_3, suggesting a greater influence of heating rate on the complete dissolution of ferrite. A similar trend was observed by Oliveira et al. [23], who attributed the increase in critical transformation temperatures with heating rate to the higher thermodynamic driving force required for diffusional transformations under continuous heating conditions. The reduced time available for the onset of the pearlite → austenite transformation demands a higher degree of superheating to provide sufficient free energy for the transformation to proceed. Consequently, both Ac_1 and Ac_3 values increase, reflecting the complex interaction between kinetic and thermodynamic effects during heating.

At higher heating rates, the diffusion of carbon atoms becomes increasingly limited, hindering both the nucleation and growth of austenite. Therefore, higher temperatures are required to enable the phase transformation. In addition, the Ac_1 and Ac_3 curves display a typical exponential decay behavior: in the initial time intervals, small decreases in heating time result in significant increases in critical transformation temperatures. However, for times shorter than approximately 100 seconds, the changes in Ac_1 and Ac_3 tends to stabilize, indicating a regime where kinetic effects become less dominant.

These results highlight the relevance of the CHT diagram as a powerful tool to accurately estimate the critical transformation temperatures Ac_1 and Ac_3, particularly in processes involving intensified thermal cycles such as Ultra-Fast Heating (UFH), welding, and hot stamping. Under such conditions, the influence of heating rate on phase transformation kinetics becomes significantly more pronounced, making many empirical equations available in the literature inadequate for predicting Ac_1 and Ac_3. These traditional relationships, although useful for slow or conventional heating conditions, often exhibit poor accuracy at higher heating rates because they neglect the kinetic effects associated with non-equilibrium transformations.

The results obtained in this study confirm this limitation. For lower heating rates, the critical temperatures exhibit small variations and remain nearly constant, indicating that empirical equations, based solely on the steel chemical composition, can still provide reasonable estimates within this range. However, at higher heating rates, a noticeable deviation of the Ac_1 and Ac_3 curves is observed.

They no longer follow a near-linear trend but instead show significant upward shifts. This behavior evidences the requirement of higher thermodynamic driving forces to promote austenite nucleation within the shorter available time.

Hence, the CHT diagram proves to be an important tool not only for characterizing the austenitizing kinetics under non-conventional heating cycles but also for supporting the optimization of modern industrial processes, where precise microstructural control is critical for achieving the desired mechanical performance in the final product.

3.2 Effect of heating rate on the Austenitic Grain Size (AGS)

Several studies have demonstrated that the heating rate has a significant effect on the austenitic grain size (AGS) in steels of different chemical compositions [9,14,18]. In general, higher heating rates tend to produce finer austenitic grains. Javaheri et al. [10] showed that, for a Nb-microalloyed low-alloy steel, a maximum heating rate of 50 °C/s resulted in remarkably small austenite grains and a highly refined final martensitic microstructure after quenching. Similarly, Liu et al. [24] reported that the austenitic grain size in a 300M steel decreased with increasing heating rate.

However, this relationship is not linear and is also influenced by other factors such as soaking temperature and the presence of alloying elements. For example, Maropoulos et al. [25] highlighted that vanadium carbides can affect grain growth, while Hu et al. [26] observed that austenite grains grow fast with increasing soaking temperature, indicating that soaking temperature plays a decisive role as well. Other authors [9] argue that the relationship between heating rate and austenitic grain size also depends on the soaking time. According to them, temperature exerts an exponential effect on AGS, whereas grain size varies proportionally to the square root of soaking time.

Figure 2 presents optical micrographs of the studied steel, subjected to subcritical oxidation to reveal the prior austenite grains. A clear qualitative trend of grain refinement with increasing heating rate can be observed. This behavior is illustrated for heating rates of 0.1 °C/s, 1 °C/s, 30 °C/s, and 50 °C/s, confirming the significant relationship between heating rate and microstructural refinement.

This behavior can be initially explained by the effect of heating rate on the nucleation stage. Increasing the heating rate decreases the critical radius of nuclei, enhancing the nucleation rate and leading to a larger number of stable nuclei entering the growth stage. The higher density of nuclei, in turn, contributes to a finer austenitic grain size. As shown in Figure 1, Ac_3 increases with heating rate, indicating a higher superheating degree and, consequently, a smaller critical radius for austenite nucleation. Moreover, as heating becomes faster, the time available for atomic diffusion, necessary for grain growth, is reduced, limiting the final grain size. In contrast, lower heating rates provide more time for diffusion, allowing grains to grow larger before the transformation is complete. Therefore, austenitic grain refinement results from both enhanced nucleation and restricted diffusion under higher heating rates.

Figure 3 illustrates the combined effect of heating rate and soaking temperature on AGS and ASTM grain number. The AGS decreases exponentially with increasing heating rate, regardless of the soaking temperature. It can also be observed that, in addition to the heating rate, the austenitizing temperature significantly influences grain growth kinetics. For example, when comparing 1150 °C and 1000 °C at a constant heating rate of 30 °C/s, lowering the soaking temperature promotes a marked grain refinement: the reduction from 1150 °C to 1000°C results in an approximately
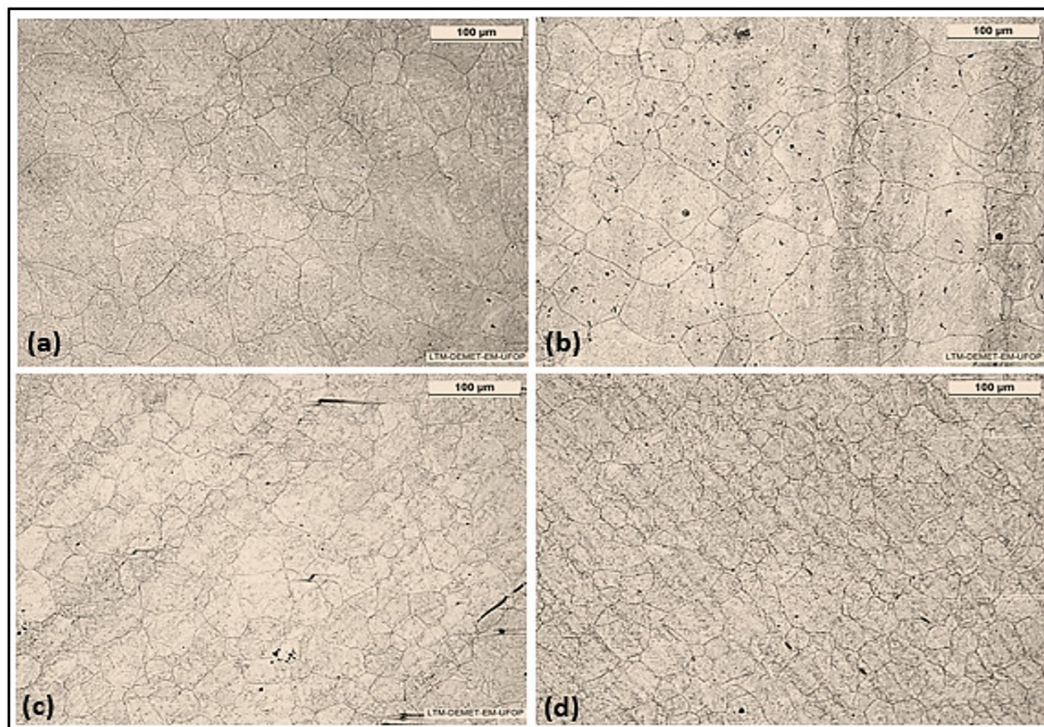

Figure 2. Comparison of prior austenite grains revealed in samples heated to 1150 °C at (a) 0.1 °C/s; (b) 1 °C/s; (c) 30 °C/s; and (d) 50 °C/s (Optical Microscopy – 200X – Subcritical Oxidation).
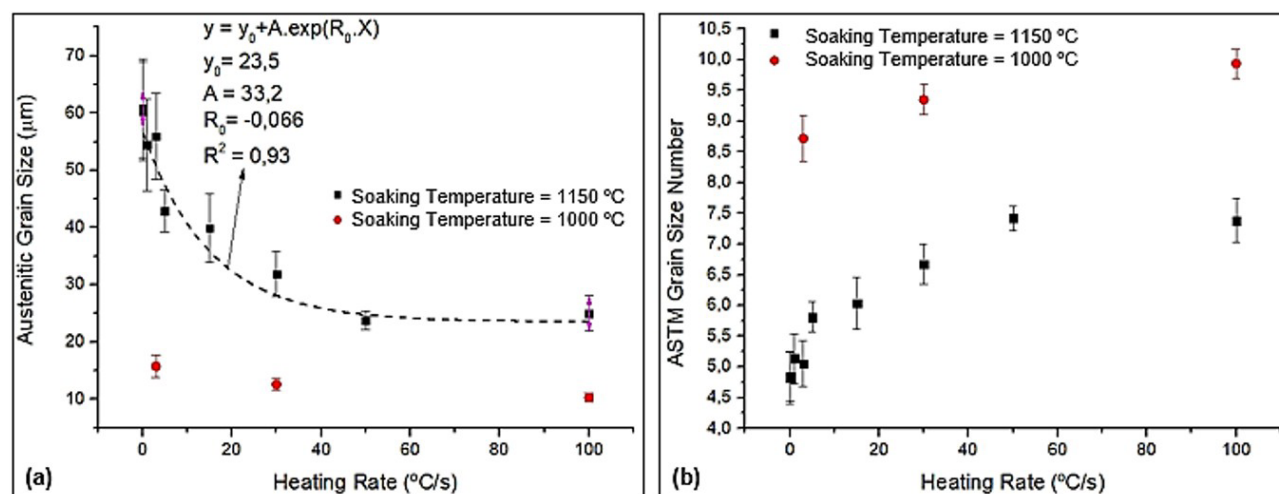
Figure 3. (a) Influence of heating rate and soaking temperature on AGS; (b) relationship between ASTM grain number and heating rate at different soaking temperatures.

60% decrease in the average austenitic grain size. This difference is particularly noteworthy because 1150 °C is far above Ac_3. The higher the soaking temperature relative to Ac_3, the greater the thermodynamic driving force for grain growth, since the critical nucleation radius is reduced and atomic diffusion becomes more intense. Consequently, the austenite grains tend to grow faster.

At lower heating rates, the difference in AGS between 1000 °C and 1150 °C becomes even more pronounced. This occurs because, under slower heating, more time is available for atomic diffusion, which favors grain growth at higher temperatures. In contrast, at higher heating rates (e.g., 100 °C/s), the effective diffusion time is much shorter. Although the thermodynamic driving force for growth increases due to superheating, the short time available limits grain coarsening.

Hence, the difference in grain size between the two soaking temperatures becomes less significant at high heating rates, highlighting the diffusion-limited nature of grain growth. This behavior underscores the importance of controlling not only heating rate but also soaking temperature for microstructural control in steels.

In this study, a predictive equation (Equation 5) was proposed to estimate the average austenitic grain size y (in μm) as a function of the heating rate X (in °C/s), considering continuous heating up to 1150 °C. The parameters were obtained by nonlinear fitting, reaching a good correlation coefficient ($R^2 = 0.93$), indicating that the model well represents the experimental data.

The fitted values were $y_0 = 23.5$ μm, $A = 33.2$ μm, and $R_0 = -0.066$ s/°C. Equation 5 reveals an exponential trend of AGS reduction with increasing heating rate, indicating that at faster heating conditions, the average grain size decreases sharply at first and then stabilizes.

$$y = y_0 + A.\exp(R_0.X) \quad (5)$$

This behavior can be interpreted as follows: at low heating rates, the transformation occurs gradually, allowing only part of the preferential nucleation sites (such as grain boundaries, dislocations, and second-phase particles) to be activated. As the heating rate increases, superheating accelerates austenite nucleation and reduces the critical nucleation radius, favoring the formation of new nuclei. However, at very high heating rates, saturation of available nucleation sites occurs; that is, nearly all favorable sites are already occupied, and the number of new nuclei tends to stabilize. Furthermore, under high heating rates, the time available for atomic diffusion is extremely limited, hindering the growth of the newly formed nuclei. Thus, even though the thermodynamic driving force is greater due to superheating, the kinetic restriction imposed by limited diffusion and nucleation-site saturation explains why AGS reduction becomes less pronounced under such conditions. This phenomenon is evident in Figure 3(a), where the differences in measured grain size at higher heating rates are small.

High soaking temperatures, such as 1150 °C, provide greater thermal energy, promoting more intense diffusion and, consequently, greater grain growth. In addition, prolonged soaking increases the available time for diffusion, leading to more significant coarsening. Conversely, when the soaking temperature is reduced to 1000 °C, the thermal energy is lower, even at the lowest heating rates, effectively restricting grain growth. As the experiments performed at 1000 °C aimed to highlight the role of diffusion during the grain growth stage, a reduced number of tests was carried out. For this reason, Equation 5 was not fitted to the experimental data obtained at this temperature.

The difference in behavior between the two soaking temperatures can also be understood by analyzing Figure 3b, which shows the ASTM grain number as a function of heating rate, in conjunction with the CHT diagram of the steel (Figure 1). The analysis of these curves indicates

that, at lower heating rates, the critical transformation temperatures (Ac_1 and Ac_3) are also lower. For instance, at 0.1 °C/s, the complete steel austenitizing occurs around 850 °C, while at 100 °C/s, Ac_3 approaches 975 °C. This means that, when heated to 1150 °C, the samples subjected to lower heating rates remain for a significantly longer time above Ac_3, i.e., within the austenite stability region. This provides more time and thermal energy for diffusion-controlled grain growth, explaining the larger grain sizes observed in these conditions. In contrast, at 1000 °C, the difference between the soaking temperature and Ac_3 is much smaller, even for the lowest heating rates. As a result, the effective time spent in the growth regime is reduced, efficiently limiting grain coarsening even when nucleation occurs under slow heating.

This behavior demonstrates the importance of the simultaneous control of heating rate and soaking temperature in processes such as UFH, especially when microstructural refinement is desired. From a practical standpoint, it is worth noting that most conventional heat treatments for steels, such as quenching, are performed at heating rates below 3 °C/s. Using this value as an industrial reference, it can be seen that, even without resorting to thermomechanical processing, the proper control of heating rate and soaking temperature can reduce the AGS from approximately 60 μm to about 10 μm. This substantial reduction in grain size, achieved solely by thermal control, is particularly relevant for thin components, where diffusion times are shorter and mechanical strength and toughness are highly sensitive to microstructural scale. The results presented in this work elucidate the mechanisms governing austenitic microstructure formation and provide valuable insights for optimizing industrial heat treatments of thin-section components.

They emphasize the potential of controlled UFH as a means to refine microstructure and consequently enhance mechanical performance through precise control of heating parameters.

4 Conclusions

The results obtained in this study clearly demonstrate that the heating rate has a direct influence on the critical transformation temperatures of the modified SAE 15B30 steel. The observed Ac_1 and Ac_3 shift toward higher values with increasing heating rate reinforces the importance of kinetic effects in phase transformations under fast heating conditions. This behavior highlights the relevance of the Continuous Heating Transformation (CHT) diagram as a valuable tool for modern industrial applications, such as Ultra-Fast Heating (UFH), where precise thermal control is essential to achieve the desired microstructures and, consequently, high mechanical performance.

With regard to the austenitic grain size, it was verified that higher heating rates promote significant grain refinement by simultaneously enhancing nucleation and restricting the time available for grain growth. The predictive equation proposed in this study exhibited a strong correlation with the experimental data ($R^2 = 0.93$), confirming the robustness of the model. However, a stabilization of the austenitic grain size was observed at very high heating rates, which can be attributed to the combined effects of nucleation-site saturation and diffusion limitation.

A remarkable decrease in the average austenitic grain size, from approximately 60 μm to about 10 μm, was achieved solely through thermal control, without any thermomechanical processing.

This finding is particularly relevant for thin-section components, where diffusion times are short and mechanical performance is highly sensitive to microstructural scale. The present study therefore emphasizes the importance of an integrated approach that considers both heating rate and soaking temperature in the design of heat treatment parameters. Such control enables the optimization of microstructure and mechanical properties while aligning with current industrial trends toward higher energy efficiency and sustainable processing routes.

Acknowledgements

References

1   Kumar K, Dixit S, Haq MZ, Vateva KM, Vatin NI, Rekha M, et al. Revolutionising heat treatment: novel strategies for augmented performance and sustainability. E3S Web of Conferences. 2023;430:01200. https://doi.org/10.1051/e3sconf/202343001200.

2   Ma S, Yang X, Fu L, Shan A. Achieving high strength-ductility synergy in nickel aluminum bronze alloy via a quenching-aging-tempering heat treatment. Materials Letters. 2023;333:133661. https://doi.org/10.1016/j.matlet.2022.133661.

3   Xi N, Tang K, Fang X, Li Y, Duan Y, Huang K. Enhanced comprehensive properties of directed energy deposited Inconel 718 by a novel integrated deposition strategy. Journal of Materials Science and Technology. 2023;141:42-55. https://doi.org/10.1016/j.jmst.2022.09.026.

4   Banis A, Papaefthymiou S. Microstructure characterization of an ultra-fast heated medium carbon chromium-manganese high strength steel. International Journal of Metallurgy and Metal Physics. 2018;3:021. https://doi.org/10.35840/2631-5076/9221.

5   Banis A, Duran EH, Bliznuk V, Sabirov L, Petrov RH, Papaefthymiou S. The effect of ultra-fast heating on the microstructure, grain size and texture evolution of a commercial low-C, medium-Mn DP steel. Metals. 2019;9(8):877. https://doi.org/10.3390/met9080877.

6   Knijf D, Puype A, Fojer C, Petrov R. The influence of ultra-fast annealing prior to quenching and partitioning on the microstructure and mechanical properties. Materials Science and Engineering A. 2015;627:198-207. https://doi.org/10.1016/j.msea.2014.12.118.

7   Han J, Yu H, Wang K, Hao B, Liu S. Study of the softening behavior of cold-rolled ribbed steel bars under ultra-fast heating. Journal of Materials Science. 2023;58(47):17873-17889. https://doi.org/10.1007/s10853-023-09127-6.

8   Tan X, Lu W, Rao X. Effect of ultra-fast heating on microstructure and mechanical properties of cold-rolled low-carbon low-alloy Q&P steels with different austenitizing temperature. Materials Characterization. 2022;191:112086. https://doi.org/10.1016/j.matchar.2022.112086.

9   Oliveira DFM, Faria GL, Moreira PS. Efeito da microestrutura prévia e da taxa de aquecimento no processo de austenitização de um aço C-Mn-Si aplicado na indústria automotiva. In: 76º Congresso Anual da ABM - Internacional; 2023; São Paulo. Anais... São Paulo: ABM; 2023. p. 2545–2558. https://doi.org/10.5151/2594-5327-39383.

10   Javaheri V, Kolli S, Grande B, Porter D. Insight into the induction hardening behavior of a new 0.40% C microalloyed steel: Effects of initial microstructure and thermal cycles. Materials Characterization. 2019;149:165-183. https://doi.org/10.1016/j.matchar.2019.01.029.

11   Meshkov YY, Pereloma EV. The effect of heating rate on reverse transformations in steels and Fe-Ni-based alloys. In: Pereloma E, Edmonds DV, editors. Phase transformations in steels: fundamentals and diffusion-controlled Transformations. Cambridge: Woodhead Publishing; 2012. p. 581-618. https://doi.org/10.1533/9780857096104.4.581.

12   Macedo MQ, Cota AB, Araújo FG. The kinetics of austenite formation at high heating rates. REM. Revista Escola de Minas. 2011;64(2):163-167. https://doi.org/10.1590/S0370-44672011000200005.

13   Settimí AG, Chukin D, Pezzato L, Gennari C, Brunelli K, Dabalá M. The impact of high heating rates on the austenitization process of 18NiCrMo5 steel. Mater Phys Mech. 2019;42(6):717-730.

14   Magalhães CHXM, Campos PHK, Faria GL. Efeito da temperatura de austenitização no tamanho de grão austenítico e nas temperaturas de início de transformação de fases em um aço do tipo TRIP 780. In: 75º Congresso da ABM; 2022; São Paulo. Anais... São Paulo: ABM; 2022. p. 58-67.

15   Gonçalves AS, Faria GL, Moreira PS. Efeito da taxa de aquecimento sobre a cinética de austenitização de um aço ao boro comercial brasileiro. In: 77º Congresso Anual da ABM - Internacional; 2024; São Paulo. Anais... São Paulo: ABM; 2024. p. 743-755. https://doi.org/10.5151/2594-5327-40570.

16   Deng YG, Li Y, Di H, Misra RDK. Effect of heating rate during continuous annealing on microstructure and mechanical properties of high-strength dual-phase steel. Journal of Materials Engineering and Performance. 2019;28(8):4556-4564. https://doi.org/10.1007/s11665-019-04253-2.

17   Valdes-Tabernero MA, Celada-Casero C, Sabirov I, Kumar A, Petrov RH. The effect of heating rate and soaking time on microstructure of an advanced high strength steel. Materials Characterization. 2019;155:109822. https://doi.org/10.1016/j.matchar.2019.109822.

18   Brooks CR. Principles of the austenitization of steels. London: Elsevier Science Publishers; 1992. 217 p.

19   Pimenta NAB, Moreira PS, Faria GL. Avaliação da formulação de reativos à base de ácido pícrico visando a revelação do grão austenítico prévio em diferentes tipos de aços. Tecnologica em Metalurgia, Materiais e Mineração. 2021;18:e2367. https://doi.org/10.4322/2176-1523.20212367.

20   Faria G, Cardoso R, Moreira P. Development of an oxidation method for prior austenite grain boundary revelation. Metallography, Microstructure, and Analysis. 2018;5(5):533-541. https://doi.org/10.1007/s13632-018-0470-1.

21   Lelis AJD. Proposição e avaliação da eficácia de um método de contraste por oxidação subcrítica para revelação de grãos austeníticos prévios em aços [monografia]. Ouro Preto: Universidade Federal de Ouro Preto; 2022.

22   American Society for Testing and Materials – ASTM. ASTM E112 – 13: Standard test method for determining average grain size. West Conshohocken: ASTM International; 2021. 28 p.

23 Oliveira FLG, Vilela JMC, Andrade MS, Cota AB. Evolução microestrutural da austenita no aquecimento contínuo de um aço de baixo carbono. In: 60º Congresso Anual da ABM; 2005; Belo Horizonte. Anais... São Paulo: ABM; 2005. p. 2272–2282. https://doi.org/10.5151/2594-5327-2005-13538-0232.

24 Liu YG, Li MQ, Dang XL. Effect of heating temperature and heating rate on austenite in the heating process of 300M steel. Materials Science Forum. 2013;749:260-267. https://doi.org/10.4028/www.scientific.net/MSF.749.260.

25 Maropoulos S, Karagiannis S, Ridley N. Factors affecting prior austenite grain size in low alloy steel. Journal of Materials Science. 2007;42(4):1309-1320. https://doi.org/10.1007/s10853-006-1191-4.

26 Hu KH, Liu XD, Feng GW, Han RD. The effect of heating process on strength and the original austenite grain size of hot forming parts. Advanced Materials Research. 2014;1063:28-31. https://doi.org/10.4028/www.scientific.net/AMR.1063.28.

Editor-in-charge:
André Luiz Vasconcellos da Costa e Silva